Multiscale Bounded Derivative Initialization for an Arbitrary Domain

G. L. BROWNING

NOAA Forecast Systems Laboratory, Boulder, and Cooperative Institute for Research in the Atmosphere, Colorado State University, Fort Collins, Colorado

H.-O. KREISS

Department of Mathematics, University of California, Los Angeles, Los Angeles, California

(Manuscript received 27 September 2000, in final form 30 October 2001)

ABSTRACT

The bounded derivative theory (BDT) for hyperbolic systems with multiple timescales was originally applied to the initialization problem for large-scale shallow-water flows in the midlatitudes and near the equator. Concepts from the theory also have been used to prove the existence of a simple reduced system that accurately describes the dominant component of a midlatitude mesoscale storm forced by cooling and heating. Recently, it has been shown how the latter results can be extended to tropospheric flows near the equator. In all of these cases, only a single type of flow was assumed to exist in the domain of interest in order to better examine the characteristics of that flow. Here it is shown how BDT concepts can be used to understand the dependence of developing mesoscale features on a balanced large-scale background flow. That understanding is then used to develop multiscale initialization constraints for the three-dimensional diabatic equations in any domain on the globe.

1. Introduction

Initialization is defined as the preparation of the initial data for a time-dependent system of ordinary or partial differential equations with multiple timescales in order to reduce the energy in the fast timescale components of the ensuing solution while maintaining good accuracy of the slowly evolving component. In the early days of meteorology, the quasigeostrophic (QG) system was used to describe large-scale midlatitude motions (Charney 1948; Phillips 1956). The QG system does not contain any high-frequency motions; that is, it is not a multiple timescale system. However, later the meteorological community began to use the primitive equations (Hinkelmann 1959; Smagorinsky 1963) that do include motions with different timescales. When observational data are used as initial values for a model based on the primitive equations (or other forecast systems with multiple timescales), large-amplitude, high-frequency gravity waves can be excited, and those waves can have a detrimental effect on the physical parameterizations in the model. In the large-scale case, it is well known that the removal of the gravity waves from the solution has little impact on the accuracy of the forecast. Thus to overcome the adverse impact of the gravity waves on the physical parameterizations in the large-scale case, a number of initialization schemes have been developed, beginning with the geostrophic approximation and balance equation (e.g., Hinkelmann 1951; Charney 1955) and proceeding to increasingly more sophisticated methods such as the nonlinear normal mode initialization method (Machenhauer 1977; Baer 1977; Baer and Tribbia 1977) and the bounded derivative method (Kreiss 1979, 1980).

In the early theories of balanced large-scale flows in the midlatitudes, the horizontal divergence was necessarily an order of magnitude smaller than the vertical component of the vorticity and all terms involving the horizontal divergence were neglected in the time-dependent equation for the horizontal divergence, resulting in the nonlinear balance equation (e.g., Browning et al. 1980). However, it has become clear that for slowly evolving smaller-scale flows in the midlatitudes and slowly evolving flows near the equator with a timescale of a day or less, the terms involving the horizontal divergence must be retained (Browning and Kreiss 1986, 1997; Browning et al. 2000). Typically the domain of interest will contain a balanced large-scale background flow and smaller-scale storms in various stages of development. It is generally believed that the majority of energy in the atmosphere is contained in the large-scale motions. However, locally mesoscale features can be dominant. Given these assumptions, a system of equations for the evolution of mesoscale features in the presence of a balanced large-scale background flow is derived. The connection of this system with previous results

Corresponding author address: Dr. Gerald Browning, NOAA/OAR/FSL, David Skaggs Research Center #3B906, 325 Broadway, Boulder, CO 80305.
E-mail: browning@fsl.noaa.gov

is discussed. In particular, an initialization scheme when both flows are present in the domain of interest will be derived.

The outline of this paper is as follows. In section 2 the solution of the three-dimensional nonlinear equations in the presence of multiple scales of heating is approximated by the sum of the balanced large-scale flow for the large-scale component of the initial conditions and heating and a residual piece. The nonlinear system describing the evolution of the residual piece is shown to be closely related to the mesoscale system described by Browning and Kreiss (1997); that is, during the timescale of the small-scale component of the heating, the dominant component of the residual piece affects the balanced large-scale solution only in the domain of the support of the small-scale heating. In section 3 a scaling of the three-dimensional equations that simultaneously describes multiple scales of motion is introduced. This scaling allows one to see how different terms vary in importance in different situations. In section 4 the scaling from section 3 is used to derive bounded derivative theory (BDT) initialization constraints for the case when multiple scales of motion are present in the domain of interest. There it can be seen how QG theory can be extended to handle the multiple-scale case. The extension of the earlier theory of the proper boundary conditions for BDT initialization constraints (Browning and Kreiss 1982) to the three-dimensional case is discussed in section 5. Numerical examples illustrating the theory are presented in section 6. The conclusions are contained in section 7.

2. Perturbations of balanced large-scale flow

For any fluid flow that has a decaying energy spectrum, the majority of the energy is contained in the low wavenumber part of the spectrum. Here it is assumed that the majority of the energy in the atmosphere is contained in balanced large-scale motions and that, though locally very important, the impact of a smaller-scale storm on the large-scale part of the energy spectrum is not immediate; that is, it takes some time before the energy in a smaller-scale storm has a significant impact on the low wavenumber part of the energy spectrum. Note that because the kinetic energy in a smaller-scale storm typically is larger than that in the local background flow, this assumption requires that smaller-scale storms not be dense over the entire globe. Under these assumptions, in this section it will be shown that a smaller-scale storm can be considered to be a perturbation on the balanced large-scale flow.

The dynamical equations describing adiabatic atmospheric motions can be written in the form (Browning and Kreiss 1986)

$$\frac{ds}{dt} = 0, \tag{2.1a}$$

$$\frac{du}{dt} + \rho^{-1}p_x - fv = 0, \tag{2.1b}$$

$$\frac{dv}{dt} + \rho^{-1}p_y + fu = 0, \tag{2.1c}$$

$$\frac{dw}{dt} + \rho^{-1}p_z + g = 0, \tag{2.1d}$$

$$\frac{dp}{dt} + \gamma p(u_x + v_y + w_z) = 0, \tag{2.1e}$$

where ρ is the density, p the pressure, $s = \rho p^{-1/\gamma}$ ($\gamma = 1.4$), $(u, v, w)^*$ is the velocity, $d/dt = \partial/\partial t + u\partial/\partial x + v\partial/\partial y + w\partial/\partial z$, $f = f_o + \beta y$ is the Coriolis parameter (in a typical midlatitude case, $f_o = 10^{-4}\ \mathrm{s}^{-1}$ and $\beta = 10^{-11}\ \mathrm{m}^{-1}\ \mathrm{s}^{-1}$), and $g = 9.8\ \mathrm{m\ s}^{-2}$ is the constant gravity acceleration.

In the original BDT scaling of the Eulerian system of equations (Browning and Kreiss 1986), the scaling parameters L_1 (U), L_2 (V), and D (W) are the representative length (velocity component) scales along the x, y, and z axes, respectively, and the dimensionless parameter S_1 represents the maximum size of the deviation of the pressure on a given height from the horizontal mean of the pressure on that height divided by the mean. In a typical midlatitude large-scale case these scaling parameters have the values

$$L_1 = L_2 = 1000\ \mathrm{km}, \qquad D = 10\ \mathrm{km}, \tag{2.2a}$$

$$U = V = 10\ \mathrm{m\ s}^{-1}, \qquad W = 0.01\ \mathrm{m\ s}^{-1},$$

$$S_1 = 10^{-2}, \tag{2.2b}$$

where the timescale $T = L_1/U$ is on the order of a day. The corresponding scaled system describing slowly evolving large-scale midlatitude motions is

$$\frac{ds}{dt} - \tilde{s}(w - H^L) = 0, \tag{2.3a}$$

$$\frac{du}{dt} + \varepsilon^{-1}(\rho_0^{-1}p_x - fv) = 0, \tag{2.3b}$$

$$\frac{dv}{dt} + \varepsilon^{-1}(\rho_0^{-1}p_y + fu) = 0, \tag{2.3c}$$

$$\frac{dw}{dt} + \varepsilon^{-6}(\rho_0^{-1}p_z + \tilde{p}p + gs) = 0, \tag{2.3d}$$

$$\frac{dp}{dt} + \varepsilon^{-1}wp_{0z} + \varepsilon^{-2}\gamma p_0(u_x + v_y + \varepsilon w_z) = 0, \tag{2.3e}$$

where $\rho_0(z)$ and $p_0(z)$ are the dimensionless horizontal means of the density and pressure, $s_0(z) = \rho_0(z)p_0(z)^{-1/\gamma}$, $\tilde{s} = -10s_{0z}/s_0$ [the factor of 10 is included to ensure that $\tilde{s}$ is $O(1)$ (Browning and Kreiss 1986)], $\tilde{p} = -p_{0z}/(\gamma\rho_0 p_0)$, ρ and p are the deviations of the density and pressure from their respective means, $s = \rho/\rho_0 - (1/\gamma)p/p_0$, $(u, v, w)^*$ is the dimensionless velocity, $d/dt = \partial/\partial t + u\partial/\partial x + v\partial/\partial y + \varepsilon w\partial/\partial z$, f is the dimensionless Coriolis parameter, g is the dimensionless constant gravity acceleration, H^L is the dimensionless large-scale heating, and $\varepsilon = 10^{-1}$. In the BDT, once a standard nondimensionalization is performed and appropriate scaling parameters are chosen for

the flow of interest, dimensionless quantities such as the Rossby number are replaced by the appropriate power of ε for application of mathematical tools. Note that the same variables have been used for both the dimensional and dimensionless systems. This should cause no confusion because in the rest of the theoretical presentation, only dimensionless variables will be used.

In general the initial data for (2.1) contains information for all three components of the solution, that is, the slowly evolving component, the gravity wave component (e.g., the large-scale gravity waves generated by mesoscale storms), and the sound wave component. To a first approximation, the latter two components satisfy known linear differential equations and can be subtracted from the solution of (2.1) following the procedures in Browning and Kreiss (1997). Because these two components of the solution currently are not accurately observed and believed not to affect the large-scale solution during a short-term large-scale forecast, they are removed from the solution by initialization or numerical methods. To ensure that the large-scale solution is free of gravity and sound waves as is the standard practice, compute the large-scale part (denoted by the superscript L) of the initial vertical component of vorticity $\zeta^L(x, y, z, 0) = -u^L_y(x, y, z, 0) + v^L_x(x, y, z, 0)$, determine the remaining large-scale dynamic variables from the bounded derivative theory large-scale diabatic initialization constraints, and replace the large-scale component of the initial conditions for (2.1) with these balanced initial conditions.

Now solve the system:

$$\frac{d_L s^L}{dt} - \tilde{s}(w^L - H^L) = 0, \tag{2.4a}$$

$$\frac{d_L u^L}{dt} + \varepsilon^{-1}(\rho_0^{-1} p^L_x - f v^L) = 0, \tag{2.4b}$$

$$\frac{d_L v^L}{dt} + \varepsilon^{-1}(\rho_0^{-1} p^L_y + f u^L) = 0, \tag{2.4c}$$

$$\frac{d_L w^L}{dt} + \varepsilon^{-6}(\rho_0^{-1} p^L_z + \tilde{p} p^L + g s^L) = 0, \tag{2.4d}$$

$$\frac{d_L p^L}{dt} + \varepsilon^{-1} w^L p_{0z} + \varepsilon^{-2}\gamma p_0 (u^L_x + v^L_y + \varepsilon w^L_z) = 0, \tag{2.4e}$$

where $d_L/dt = \partial/\partial t + u^L \partial/\partial x + v^L \partial/\partial y$, using the balanced large-scale initial conditions to obtain an approximation of the evolution of the balanced large-scale solution. Then write the solution of (2.3) as the sum of the solution of (2.4) and a residual variable (denoted by the superscript R), for example, $s = s^L + s^R$. Substituting these expressions into (2.3), the time-dependent nonlinear system for the residual variables is

$$\frac{d_R s^R}{dt} + I(s) - \tilde{s} w^R = \varepsilon F(s), \tag{2.5a}$$

$$\frac{d_R u^R}{dt} + I(u) + \varepsilon^{-1}(\rho_0^{-1} p^R_x - f v^R) = \varepsilon F(u), \tag{2.5b}$$

$$\frac{d_R v^R}{dt} + I(v) + \varepsilon^{-1}(\rho_0^{-1} p^R_y + f u^R) = \varepsilon F(v), \tag{2.5c}$$

$$\frac{d_R w^R}{dt} + I(w) + \varepsilon^{-6}(\rho_0^{-1} p^R_z + \tilde{p} p^R + g s^R) = \varepsilon F(w), \tag{2.5d}$$

$$\frac{d_R p^R}{dt} + I(p) + \varepsilon^{-1} w^R p_{0z} + \varepsilon^{-2}\gamma p_0 (u^R_x + v^R_y + \varepsilon w^R_z) = \varepsilon F(p), \tag{2.5e}$$

where $d_R/dt = \partial/\partial t + (u^L + u^R)\partial/\partial x + (v^L + v^R)\partial/\partial y + \varepsilon(w^L + w^R)\partial/\partial z$, $I(q) = (u^R q^L_x + v^R q^L_y + \varepsilon w^R q^L_z)$ is a linear combination of the undifferentiated unknown velocity components, and $F(q) = -w^L q^L_z$ is a large-scale forcing term.

Given the assumption that the large-scale component of the initial conditions for (2.1) is balanced, the large-scale component of the initial conditions for (2.5) is zero and the small-scale component is the same as the small-scale component of the initial conditions for (2.1). Because the initial conditions for (2.5) are of small horizontal spatial scale and the forcing terms do not play a significant role in the solution for several hours, the appropriate scaling parameters are

$$L_1 = L_2 = 100 \text{ km}, \qquad D = 10 \text{ km}, \tag{2.6a}$$

$$U = V = 10 \text{ m s}^{-1}, \qquad W = 1 \text{ m s}^{-1}, \qquad S_1 = 10^{-3}, \tag{2.6b}$$

where the timescale is on the order of a few hours (Browning and Kreiss 1997). By comparing (2.6) with (2.2), it can be seen that this scaling for the unknown variables with superscript R can be accomplished by making the change of independent variables

$$t = \varepsilon t', \qquad x = \varepsilon x', \qquad y = \varepsilon y',$$

and the change of dependent variables

$$p^R = \varepsilon p', \qquad s^R = \varepsilon s', \qquad w^R = \varepsilon^{-2} w'$$

in (2.5). Then the dimensionless system that describes mesoscale perturbations of balanced large-scale flow is

$$\frac{ds'}{dt} + I(s) - \varepsilon^{-2}\tilde{s}(w' - H^S) = \varepsilon F(s), \tag{2.7a}$$

$$\frac{du^R}{dt} + \varepsilon I(u) + \rho_0^{-1} p'_{x'} - f v^R = \varepsilon^2 F(u), \tag{2.7b}$$

$$\frac{dv^R}{dt} + \varepsilon I(v) + \rho_0^{-1} p'_{y'} + f u^R = \varepsilon^2 F(v), \tag{2.7c}$$

$$\frac{dw'}{dt} + \varepsilon^3 I(w) + \varepsilon^{-2}(\rho_0^{-1} p'_z + \tilde{p} p' + g s') = \varepsilon^4 F(w), \tag{2.7d}$$

$$\frac{dp'}{dt} + I(p) + \varepsilon^{-3}[w' p_{0z} + \gamma p_0 (u^R_{x'} + v^R_{y'} + w'_z)] = \varepsilon F(p), \tag{2.7e}$$

where $d/dt = \partial/\partial t' + (u^L + u^R)\partial/\partial x' + (v^L + v^R)\partial/\partial y' + (\varepsilon^2 w^L + w')\partial/\partial z$, $I(q) = u^R q_x^L + v^R q_y^L + \varepsilon^{-1} w' q_z^L$, and $F(q) = -w^L q_z^L$. Note that the change of independent variables is not applied to the known large-scale $O(1)$ coefficients and that the small-scale component of the heating has been added following earlier results (Browning and Kreiss 1986; Browning and Kreiss 1997). In previous papers where the main interest was in gravity waves, the velocity coefficients in the advective terms with superscript R can be ignored. However, when there is a collection of storms, one cannot assume that the large-scale velocity coefficients are constant and then it is necessary to solve (2.7). But for mesoscale features the same balance between the vertical velocity and heating also is present in (2.7) and to first approximation the dominant component of the solution for the general case satisfies the reduced system

$$\frac{du^R}{dt} + H^S u_z^L + \rho_0^{-1} p'_{x'} - f v^R = 0, \qquad (2.8a)$$

$$\frac{dv^R}{dt} + H^S v_z^L + \rho_0^{-1} p'_{y'} + f u^R = 0, \qquad (2.8b)$$

$$H^S p_{0z} + \gamma p_0 (u_{x'}^R + v_{y'}^R + H_z^S) = 0, \qquad (2.8c)$$

where $d/dt = \partial/\partial t' + (u^L + u^R)\partial/\partial x' + (v^L + v^R)\partial/\partial y' + H^S\partial/\partial z$. Note that the terms that are a product of the heating and vertical shear are $O(1)$ forcing terms.

Browning and Kreiss (1997) subtracted the solution of the reduced system (2.8) from the solution of (2.7) (in the simpler case mentioned above) to show that the residual part of the solution satisfies a forced linear gravity wave equation. By subtracting both of these components of the solution from the solution of (2.7), it was established that the gravity waves generated by a mesoscale storm driven by prescribed cooling and heating do not significantly interact with the dominant component of the storm. And though this theory shows that the gravity waves that are generated have very little kinetic energy compared to the dominant component in the neighborhood of the storm, it is still possible that these large-spatial-scale gravity waves have some role in initiating new storms some distance from their source. As mentioned earlier, it is common practice in global numerical weather prediction models to prepare the initial data or use numerical techniques (e.g., time filters) to suppress any gravity waves that would be generated by imbalances in the large-scale observational data. Because global models are used to provide time-dependent boundary conditions for high-resolution nonhydrostatic limited-area forecast models, this absence of gravity wave information in the boundary data can lead to a conflict between the balanced boundary conditions provided by a global model and the gravity waves generated by small-scale heat sources in the interior of the limited-area domain when those gravity waves encounter a boundary of the domain of the limited-area forecast. [This is essentially the same problem as in a two-way interacting nested model where a feature is better resolved in the fine mesh than in the coarse mesh (Browning et al. 1973)]. This problem (and the similar problem encountered when a small-scale storm encounters the boundary) can be masked by the use of numerical dissipation, but at the expense of numerical accuracy. If the energy in the gravity wave component of a mesoscale storm is sufficiently small and the mesoscale heating is confined to the interior of the limited area domain during the forecast, the use of balanced global model boundary data will not lead to a significant loss of forecast accuracy or to large amplitude discontinuities at the boundaries. If the reduced system (2.8) is used in the limited area, no large-scale gravity waves will be generated and it is only necessary to ensure that the mesoscale heating is confined to the interior of the limited-area domain to avoid boundary data conflicts. These issues will be addressed in detail in a forthcoming paper.

3. Midlatitude multiscale scaling

The first step in the application of the BDT is to scale the time-dependent system according to the properties of the slowly evolving motions of interest (Browning et al. 1980). In the original application of the BDT to the system of partial differential equations describing all atmospheric motions, the system was scaled in a general manner that was applicable to slowly evolving atmospheric motions of any length scale (Browning and Kreiss 1986). The general set of slowly evolving atmospheric motions can be divided into two cases. One case comprises those motions where the forcing term in the entropy (or potential temperature) equation is the same order of magnitude as the horizontal advection terms in that same equation. The other case is where the forcing term in the entropy equation is an order of magnitude or more larger than the horizontal advection terms in that equation. Large-scale midlatitude motions fall into the first case (Browning and Kreiss 1986), but smaller-scale midlatitude and all equatorial flows fall into the second case (Browning and Kreiss 1997; Browning et al. 2000). In the second case, gravity waves that have the same timescale as the dominant component can be generated by the longwave part of the heating. However, the length scale of the gravity waves is an order of magnitude larger than that of the dominant component and this fact must be kept in mind when trying to initialize limited-area models based on the nonhydrostatic system. As shown in the previous section, initialization constraints for the large-scale part of the initial data can be derived and the resulting large-scale balanced solution subtracted from the solution of the full system. Then initialization constraints for system (2.7) that describes the residual part of the solution can be determined. This two step process can also be combined into a single step in order to avoid the solution of two elliptic equations for the pressure at every vertical level. To better understand how the BDT can be

used to initialize the solution when motions from both cases are present in the domain of interest (the most likely case in practice), a single scaling that can be used to describe typical flows from both cases will be introduced. (In the following section this multiscale scaling will be used to derive the one-step initialization scheme.)

In the BDT, scaled systems corresponding to different motions typically will have different powers of ε in front of each of the off-diagonal terms, for example, compare (2.3) and (2.7). However, using parameters for the exponents of ε, it is possible to combine two (or more) scaled systems into a single one (this would be equivalent to letting the Rossby number vary in the domain of interest). In this vein consider the scaled system

$$\frac{ds}{dt} - \varepsilon^{-2+2n}\tilde{s}(w - H) = 0, \tag{3.1a}$$

$$\frac{du}{dt} + \varepsilon^{-n}(\rho_0^{-1}p_x - fv) = 0, \tag{3.1b}$$

$$\frac{dv}{dt} + \varepsilon^{-n}(\rho_0^{-1}p_y + fu) = 0, \tag{3.1c}$$

$$\frac{dw}{dt} + \varepsilon^{-2-4n}(\rho_0^{-1}p_z + \tilde{p}p + gs) = 0, \tag{3.1d}$$

$$\frac{dp}{dt} + \varepsilon^{-3+2n}wp_{0z} + \varepsilon^{-3+n}\gamma p_0(u_x + v_y + \varepsilon^n w_z) = \varepsilon^{-2+2n}G, \tag{3.1e}$$

where $d/dt = \partial/\partial t + u\partial/\partial x + v\partial/\partial y + \varepsilon^n w\partial/\partial z$, and the remaining dimensionless variables are as described in the previous section. Here $n = 1$ for the large-scale case and $n = 0$ for the mesoscale case. The $O(1)$ heating terms H and G are assumed to be slowly varying functions of the independent variables [for a discussion of the validity of this assumption see Browning and Kreiss (1997)]. Because the heating term G does not affect the arguments to follow, for simplicity of presentation it will be neglected.

4. Multiscale initialization constraints

The appropriate initialization constraints to ensure that the solution will be slowly evolving in time can be determined from the BDT requirement that a number of the time derivatives of the scaled system at the initial time be of order unity (Browning et al. 1980). This continues to be true when multiple scales are present in the domain of interest, but then the timescale can vary from location to location and one must be careful to ensure that time derivatives of a given order are locally of order unity. To see how this works in practice, let us apply this requirement to system (3.1). The first-order time derivative of system (3.1) will be of order unity if and only if

$$w - H = \varepsilon^{2-2n}\tilde{s}^{-1}\frac{ds}{dt} = O(\varepsilon^{2-2n}), \tag{4.1a}$$

$$\rho_0^{-1}p_x - fv = -\varepsilon^n\frac{du}{dt} = O(\varepsilon^n), \tag{4.1b}$$

$$\rho_0^{-1}p_y + fu = -\varepsilon^n\frac{dv}{dt} = O(\varepsilon^n), \tag{4.1c}$$

$$\rho_0^{-1}p_z + \tilde{p}p + gs = -\varepsilon^{2+4n}\frac{dw}{dt} = O(\varepsilon^{2+4n}), \tag{4.1d}$$

$$\varepsilon^n wp_{0z} + \gamma p_0(u_x + v_y + \varepsilon^n w_z) = -\varepsilon^{3-n}\frac{dp}{dt} = O(\varepsilon^{3-n}). \tag{4.1e}$$

When a right-hand side of one of the equations of (4.1) is small and to first approximation can be neglected, a BDT initialization constraint is obtained for the corresponding motion. The constraint obtained by neglecting the right-hand side of (4.1a) is accurate only for the mesoscale ($n = 0$). The quasigeostrophic constraints obtained from (4.1b) and (4.1c) are only accurate for the large scale ($n = 1$). Hydrostatic balance obtained by neglecting the right-hand side of (4.1d) is accurate for both (2.3) and (2.7), but not for smaller scales of motion. The constraint obtained from (4.1e) is accurate for all scales of motion. Thus in this form of the equations the choice of a reasonable set of constraints for flows from both cases is not clear. However, consider the change of variable suggested by the mesoscale case; that is, define the new variable w' by the relation

$$w = H + \varepsilon^{2-2n}w'. \tag{4.2}$$

In terms of this new variable (3.1) becomes

$$\frac{ds}{dt} - \tilde{s}w' = 0, \tag{4.3a}$$

$$\frac{d\zeta}{dt} + \delta\zeta + \varepsilon^n(w_x v_z - w_y u_z) + \varepsilon^{-n}(f\delta + f_y v) = 0, \tag{4.3b}$$

$$\frac{d\delta}{dt} + \delta^2 - 2J + \varepsilon^n(w_x u_z + w_y v_z) + \varepsilon^{-n}(\rho_0^{-1}\nabla^2 p - f\zeta + f_y u) = 0, \tag{4.3c}$$

$$\varepsilon^{2-2n}\frac{dw'}{dt} + \frac{dH}{dt} + \varepsilon^{-2-4n}(\rho_0^{-1}p_z + \tilde{p}p + gs) = 0, \tag{4.3d}$$

$$\frac{dp}{dt} + \varepsilon^{-3+2n}(H + \varepsilon^{2-2n}w')p_{0z} + \varepsilon^{-3+n}\gamma p_0[\delta + \varepsilon^n(H_z + \varepsilon^{2-2n}w')_z] = 0, \tag{4.3e}$$

where $J = u_x v_y - u_y v_x$ and the variables $\zeta = -u_y + v_x$ and $\delta = u_x + v_y$ have been introduced in order to simplify the derivation of the constraints (Browning and Kreiss 1987). Now (4.3e) yields the requirement

$$\delta = -\varepsilon^n[H + \varepsilon^{2-2n}w')_z + (\gamma p_0)^{-1}(H + \varepsilon^{2-2n}w')p_{0z}] + O(\epsilon^{3-n}), \quad (4.4a)$$

that is accurate for all scales of motion and ensures that the constraint from (4.3b) is satisfied [recall that $f_y = O(\varepsilon)$ for the large-scale case]. The requirement that arises from (4.3c) is

$$\nabla^2 p = \rho_0\left\{f\zeta - f_y u - \varepsilon^n\left[\frac{d\delta}{dt} + \delta^2 - 2J + \varepsilon^n(w_x u_z + w_y v_z)\right]\right\}. \quad (4.4b)$$

For the large scale case ($n = 1$), to first approximation this is just the linear balance equation of quasigeostrophic theory (Charney 1948). However, when flows from the second case are present, for example, when $n = 0$, all terms must be retained [the extra terms can be determined from the heating using (4.2) and (4.4a)]. Note that if the two step initialization process is used, first the linear balance equation is solved on each vertical level to balance the initial conditions for the large-scale flow and then a second elliptic equation on each level is solved to balance the initial conditions for the small-scale flow. These two steps are combined in the one-step procedure.

The time derivative of w' is of order unity if and only if

$$\rho_0^{-1}p_z + \tilde{p}p + gs = -\varepsilon^{2+4n}\frac{dH}{dt} + O(\varepsilon^{4+2n}). \quad (4.4c)$$

Thus for the large-scale and mesoscale cases, hydrostatic balance is accurate. For the smaller-scale cases, hydrostatic equilibrium can be replaced by an inhomogeneous version of the hydrostatic equation.

The only dynamical variable that can be used to represent the slowly evolving solution for all scales of motion anywhere on the globe is the vertical component of vorticity [for a discussion of an alternative in the midlatitudes see Browning et al. (1980)]. Therefore assume that at a given time the vertical component of the vorticity ζ is given and H and H_t are known (e.g., from observations or a physical parameterization). The divergence is known up to an error term $O(\varepsilon)$ from (4.4a). (In the large-scale case the entire right-hand side can be neglected and in the mesoscale case the w' terms can be neglected.) Then the horizontal velocity components u and v can be determined up to an error term $O(\varepsilon)$ (Browning et al. 1980). Subsequently the balanced pressure can be determined from (4.4b) up to an error term $O(\varepsilon)$ and then s (or the potential temperature) to the same degree of accuracy from (4.4c). The only remaining variable is w, which is known quite accurately for flows from the second case but not for the large-scale case. As in previous applications of the BDT (Browning et al. 1980), requiring additional time derivatives to be of order unity leads to additional and/or refined constraints. To simplify the presentation, in the following derivation it is assumed that f is constant and that $\tilde{p} = 0$. Then following the derivation of the ω equation in the quasigeostrophic theory (Charney 1948), first differentiate the large-scale version of (4.4b) with respect to z and use hydrostatic balance to obtain

$$-g\rho_0\nabla^2 s = f(\rho_0\zeta)_z. \quad (4.5)$$

Applying the operator $d_h/dt = \partial/\partial t + u(\partial/\partial x) + v(\partial/\partial y)$ to this equation, (4.5) becomes

$$-g\rho_0\left[\nabla^2\frac{d_h s}{dt} - C_2\right] = f\left[\left(\rho_0\frac{d_h\zeta}{dt}\right)_z - C_1\right]. \quad (4.6a)$$

The commutators C_1 and C_2 are defined by

$$C_1 = \frac{\partial}{\partial z}\left[\frac{d_h}{dt}(\rho_0\zeta)\right] - \frac{d_h}{dt}\left[\frac{\partial}{\partial z}(\rho_0\zeta)\right] = u_z(\rho_0\zeta)_x + v_z(\rho_0\zeta)_y, \quad (4.6b)$$

$$C_2 = \nabla^2\frac{d_h s}{dt} - \frac{d_h}{dt}\nabla^2 s = u_{xx}s_x + 2u_x s_{xx} + u_{yy}s_x + 2u_y s_{xy} + v_{xx}s_y + 2v_x s_{xy} + v_{yy}s_y + 2v_y s_{yy}. \quad (4.6c)$$

Now replacing $d_h s/dt$ and $d_h\zeta/dt$ using (3.1a) and (4.3b), (4.6) becomes

$$-\varepsilon^{-2+2n}g\rho_0\tilde{s}\nabla^2(w - H) + f^2(\rho_0\delta)_z = R_1, \quad (4.7a)$$

where

$$R_1 = -g\rho_0 C_2 - fC_1, \quad (4.7b)$$

and on rearranging the terms slightly the elliptic equation for w is

$$\varepsilon^{-2+2n}\nabla^2(\rho_0 w) + f^2(g\tilde{s})^{-1}(\rho_0 w)_{zz} = \varepsilon^{-2+2n}\rho_0\nabla^2 H - (g\tilde{s})^{-1}R_1. \quad (4.8)$$

If the heating is broken into its large- and small-scale components, to first approximation (4.8) yields $w^R = H^S + O(\varepsilon^2)$ in the domain of the small-scale heating as required for slowly evolving solutions of (2.7). And outside of the domain of the small-scale heating, (4.8) reduces to the traditional elliptic equation for the vertical velocity. In that region note that (4.8) basically ensures that the second derivative of the horizontal divergence δ will be of order unity.

5. Boundary conditions for the initialization constraints

An important part of the BDT for hyperbolic systems with multiple timescales is the derivation of boundary conditions for the elliptic initialization constraints from the boundary conditions for the initial-boundary value problem for the hyperbolic system. This consistency mathematically ensures that the solution will be slowly

evolving in time even in the presence of open boundaries. To see how this compatibility is achieved for the three-dimensional diabatic system, consider (3.1) in the domain $x \geq 0$, $0 \leq y \leq 1$, $0 \leq z \leq 1$ with an open boundary at $x = 0$, periodicity in y, and solid walls at $z = 0$ and $z = 1$. Numerous well-posed boundary conditions with different physical properties exist, but here it is convenient to assume that the one-dimensional inflow characteristic variables at an open boundary are known because that automatically guarantees the well-posedness of the initial boundary value problem (Browning and Kreiss 1982). In the domain above, if the normal velocity at $x = 0$ is directed into the domain, that is, if $u(0, y, z, t) > 0$, then the incoming characteristic variables are s, $u + \varepsilon^{3/2-n}p/\sqrt{\gamma p_0 \rho_0}$, v, and w, but if the normal velocity at $x = 0$ is directed out of the domain, that is, if $u(0, y, z, t) < 0$, then the only incoming characteristic variable is $u + \varepsilon^{3/2-n}p/\sqrt{\gamma p_0 \rho_0}$. Thus the only characteristic variable that can be guaranteed to be present at a given boundary point at $x = 0$ at a given point in time is the variable $u + \varepsilon^{3/2-n}p/\sqrt{\gamma p_0 \rho_0}$, which to first approximation is just the normal velocity u (Browning and Kreiss 1982). [For the large-scale case $n = 1$, this is only accurate to $O(\varepsilon^{1/2})$, but it can be iterated to provide higher accuracy if necessary.] Given the normal velocity u at $x = 0$, it is possible to solve the Helmholtz equations

$$\nabla^2 u = -\zeta_y + \varepsilon^n \delta_x, \quad \text{and} \tag{5.1a}$$

$$\nabla^2 v = \zeta_x + \varepsilon^n \delta_y, \tag{5.1b}$$

for u and v at each vertical level by using the additional boundary condition

$$v_x(0, y, z, t) = u_y(0, y, z, t) + \zeta(0, y, z, t), \tag{5.2}$$

for v. [The horizontal divergence can be determined from (4.4a) using the initial vorticity and heating data as discussed in the previous section.] Also, it is possible to solve (4.1b) for the normal derivative of p at $x = 0$:

$$p_x = f\rho_0 v - \varepsilon^n \rho_0 \frac{d_h u}{dt}, \tag{5.3}$$

which provides a boundary condition for (4.4b). Equation (4.4c) for s does not require a lateral boundary condition, but the elliptic equation (4.8) for w does. Differentiating (5.3) with respect to z and using the hydrostatic approximation, (5.3) becomes

$$-g\rho_0 s_x = f(\rho_0 v)_z - \varepsilon^n \rho_0 \left(\frac{d_h u}{dt}\right)_z - \varepsilon^n \rho_{0z} \frac{d_h u}{dt}. \tag{5.4}$$

As in the derivation of the ω equation, apply the operator d_h/dt to (5.4) to obtain

$$-g\rho_0 \left[\left(\frac{d_h s}{dt}\right)_x - C(x, s)\right] = R_2, \tag{5.5}$$

where

$$R_2 = f\left\{\left[\frac{d_h(\rho_0 v)}{dt}\right]_z - C(z, \rho_0 v)\right\} - \varepsilon^n \rho_0 \frac{d_h}{dt}\left(\frac{d_h u}{dt}\right)_z - \varepsilon^n \rho_{0z} \frac{d_h}{dt}\left(\frac{d_h u}{dt}\right)$$

and the commutator $C(d, q)$ is defined by

$$C(d, q) = \frac{\partial}{\partial s}\left(\frac{d_h q}{dt}\right) - \frac{d_h}{dt}\left(\frac{\partial q}{\partial s}\right) = u_d q_x + v_d q_y.$$

Replacing $d_h s/dt$ using (2.3a), the Neumann boundary condition

$$(\rho_0 w)_x = \rho_0 H_x + (g\tilde{s})^{-1}[g\rho_0 C(x, s) - R_2] \tag{5.6}$$

for the elliptic equation (4.8) for w is obtained.

6. Numerical examples

It is common in practice to initially run a global numerical weather prediction model based on the primitive equations to provide a forecast of large-scale features for several days and large-scale boundary data for fine mesh limited-area models that are located over areas of developing smaller-scale features. Here the effectiveness of BDT multiscale initialization can be demonstrated in a similar setting using the following combination of numerical models. A channel model (periodic boundary conditions in x and solid walls at the remaining boundaries) will be used as a representative of a global model. The use of solid walls in the y direction allows for the dependence of the balanced initial conditions on the variation of the Coriolis factor without the complications of spherical geometry. A model with accurate and stable open boundary conditions in x and solid walls at the remaining boundaries will be used as a representative of a limited-area model (see detailed discussion of numerical approximations used in this model in the appendix). The initial data for the channel model will be obtained by applying the channel version of the BDT initialization package to a specified initial streamfunction representing a typical large-scale flow pattern. During the subsequent channel forecast, a specified mesoscale heating will be turned on in a typical area of the large-scale pattern. Although the channel model can accurately depict the large-scale flow in the absence of the mesoscale heating with a relatively coarse mesh, it was run with a sufficiently fine mesh ($\Delta x = \Delta y = 12.5$ km, $\Delta z = 1$ km) to resolve both the large-scale and mesoscale flows to provide a sufficiently accurate channel solution of the forced problem. The maximum of the mesoscale heating occurs at $t = 6$ h. The initial data for the limited-area model will be obtained by applying the limited-area version of the BDT initialization package to the multiscale vorticity from the channel model at $t = 3$ h, that is, at the developing stage of the mesoscale storm. Note that to balance the flow at this period of time for the limited-area model requires

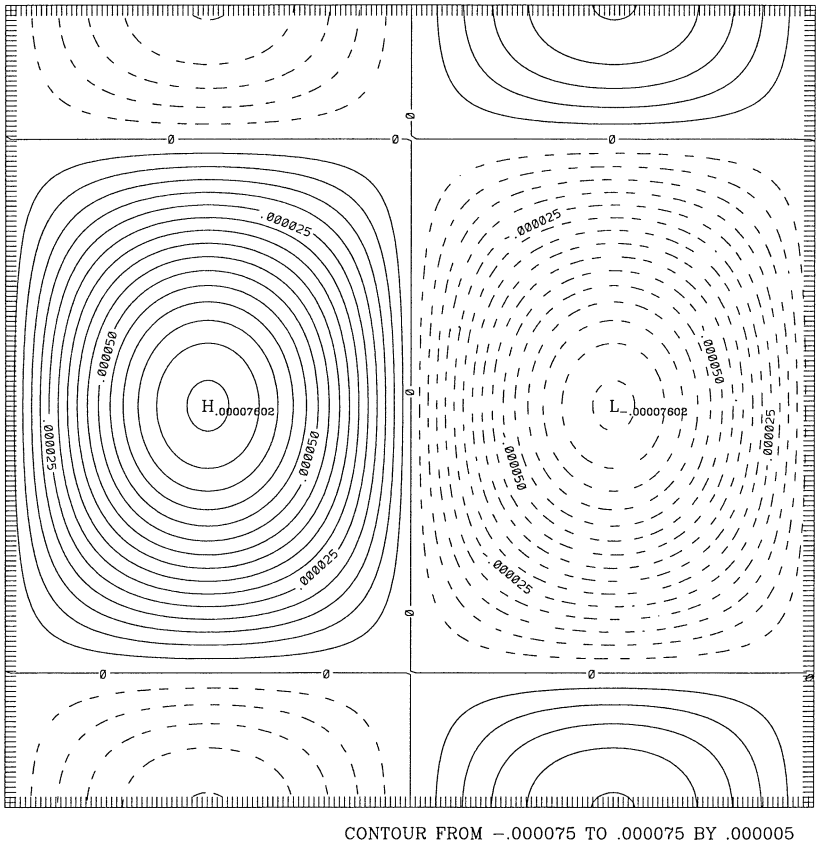

FIG. 1. The channel model vertical component of vorticity ζ at $z = 3$ km and $t = 0$ h. The length of a side of the square domain is 2000 km and the contour interval is 5×10^{-6} s^{-1}.

both the mesoscale vorticity and heating. [In this paper the mesoscale heating will be a specified mathematical function in order to demonstrate the theory in a simple setting. However, the limited-area BDT initialization package was originally developed for the Air Force Office of Scientific Research using high-resolution Offut Air Force Base aviation (AVN) vorticity data and the Kuo parameterization scheme.] It will be shown that both the channel and limited-area model solutions evolve slowly in time and that the limited-area model reproduces the multiscale channel solution very accurately.

The original streamfunction used as the starting point for the channel model initialization procedure was

$$\psi = -(2\pi)^{-1}u_1 Y \sin(2\pi x/X)[1 - \cos(2\pi y/Y)] \times [\sin(\pi z/z_T) + 0.1], \quad (6.1a)$$

where X and Y are the lateral dimensions of the domain, z_T is the top of the model domain, and $u_1 = 10$ m s^{-1}. The channel model was run in a domain with $X = Y =$ 2000 km and $z_T = 12$ km. Thus the horizontal part of this streamfunction represents a large-scale high pressure center followed by a large-scale low pressure center. The basic horizontal pattern is multiplied by half a sine wave in the vertical direction plus a constant to ensure that the pattern is also present at the surface and top of the model domain. At the suggestion of John Brown (NOAA Forecast Systems Laboratory) the mean wind profile

$$\bar{u}(z) = 5 + 10 \sin(0.75\pi z/z_T) \quad (6.1b)$$

was added to the value for $u(-\psi_y)$ obtained from (6.1a) in order to obtain a more realistic mean wind profile. The 5 m s^{-1} constant wind ensures that $u(x, y, z, 0) > 0$ so that the western boundary is an inflow boundary and the eastern boundary is an outflow boundary. This makes it possible to distinguish any problems that are peculiar to one or the other type of flow at the boundaries. Figure 1 shows the initial large-scale vertical component of vorticity corresponding to (6.1) at $z = 3$ km for the channel model. In both numerical models, the mean atmospheric profiles were based on an isothermal atmosphere at rest ($T_0 = 300$ K) and the Coriolis parameter midlatitude values ($f_0 = 10^{-4}$ s^{-1} and $\beta = 10^{-11}$ m^{-1} s^{-1}). For these values, the balanced initial fields p and w at $z = 3$ km obtained by solving the BDT elliptic constraints (4.4b) and (4.8) with the appropriate boundary conditions for the channel taken from section 5 are

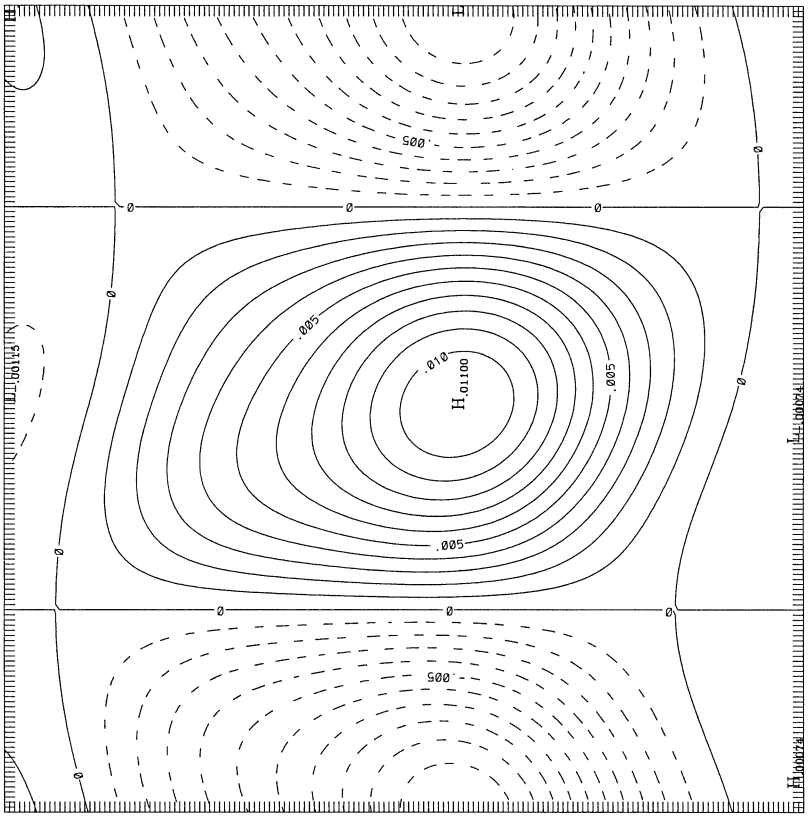

FIG. 3. The channel model balanced vertical velocity w at $z = 3$ km and $t = 0$ h. The length of a side of the square domain is 2000 km and the contour interval is 0.001 m s^{-1}.

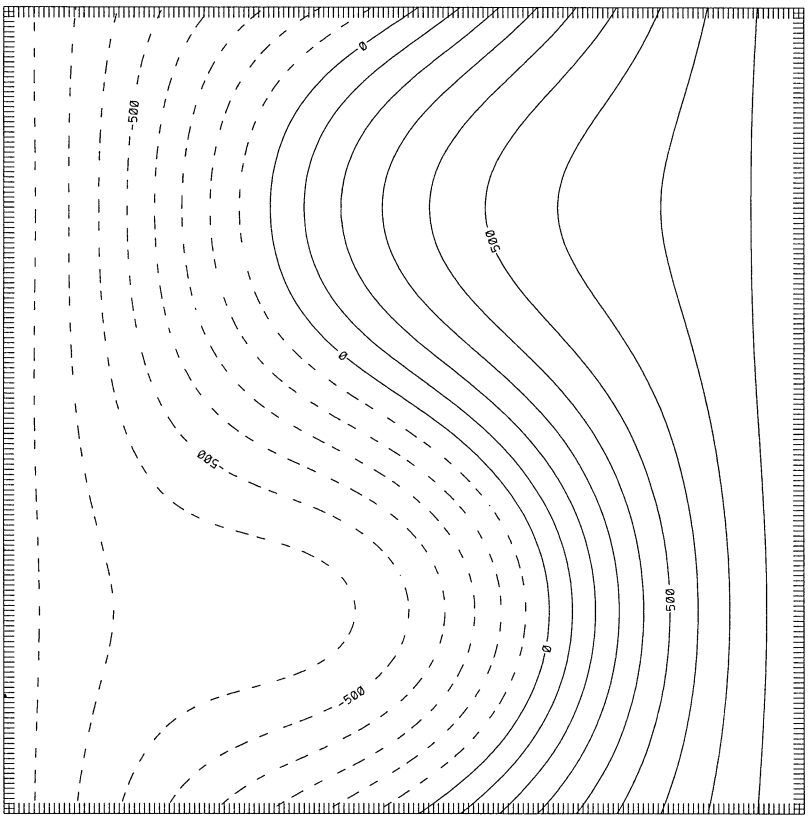

FIG. 2. The channel model balanced pressure p at $z = 3$ km and $t = 0$ h. The length of a side of the square domain is 2000 km and the contour interval is 100 kg m^{-1} s^{-2}.

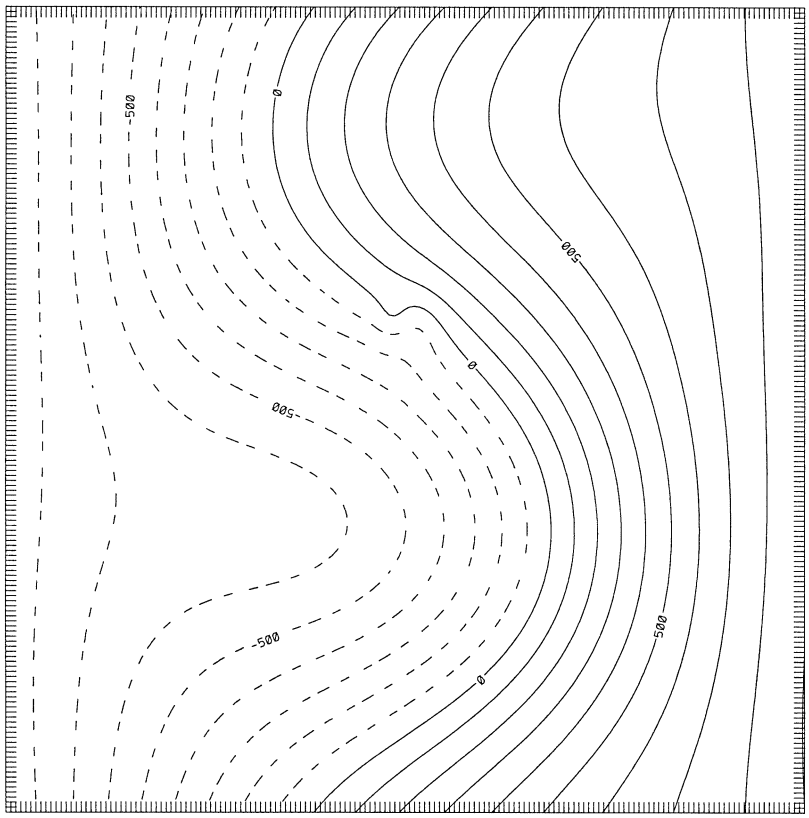

FIG. 5. The channel model pressure p at $z = 3$ km and $t = 6$ h. The length of a side of the square domain is 2000 km and the contour interval is 100 kg m^{-1} s^{-2}.

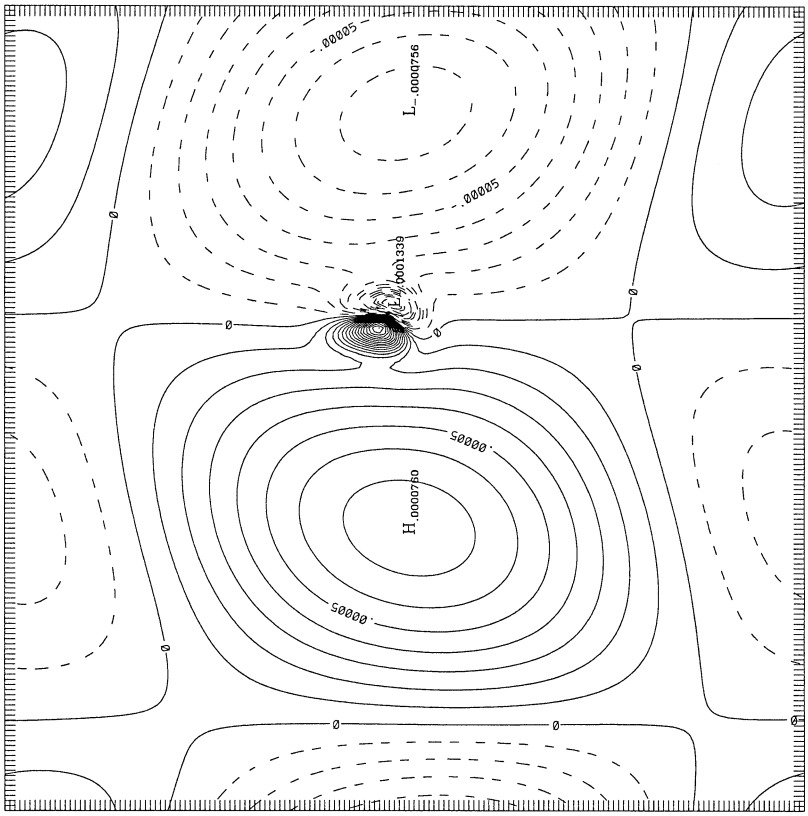

FIG. 4. The channel model vertical component of vorticity ζ at $z = 3$ km and $t = 6$ h. The length of a side of the square domain is 2000 km and the contour interval is 10^{-5} s^{-1}.

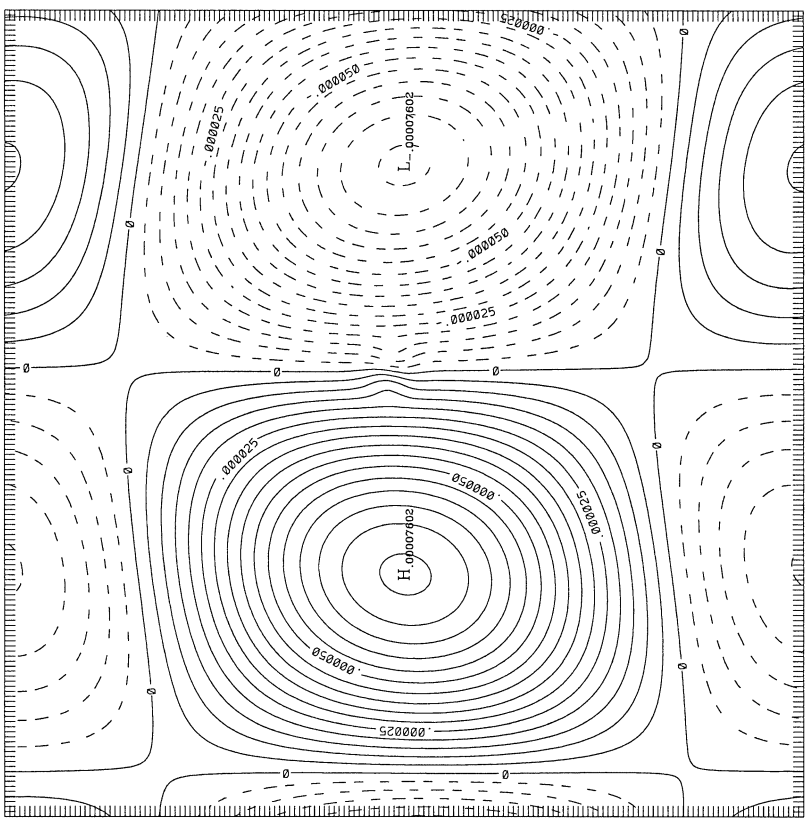

FIG. 6. The channel model vertical velocity w at $z = 3$ km and $t = 6$ h. The length of a side of the square domain is 2000 km and the contour interval is 0.04 m s^{-1}.

FIG. 7. The channel model vertical component of vorticity ζ at $z = 3$ km and $t = 3$ h. The length of a side of the square domain is 2000 km and the contour interval is 5×10^{-6} s^{-1}.

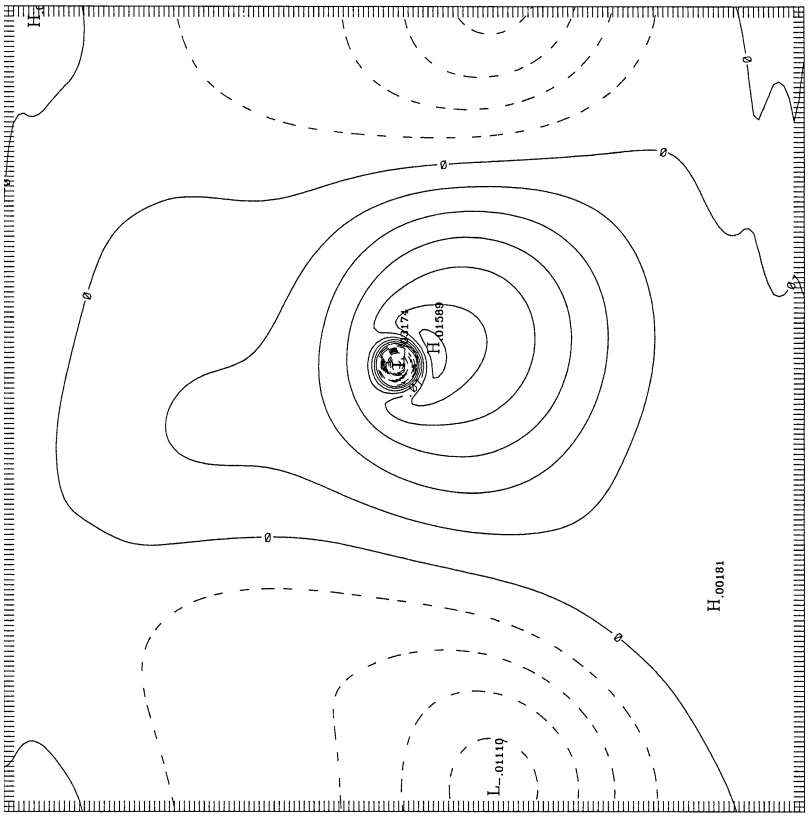

FIG. 9. The channel model vertical velocity w at $z = 3$ km and $t = 3$ h. The length of a side of the square domain is 2000 km and the contour interval is 0.0025 m s^{-1}.

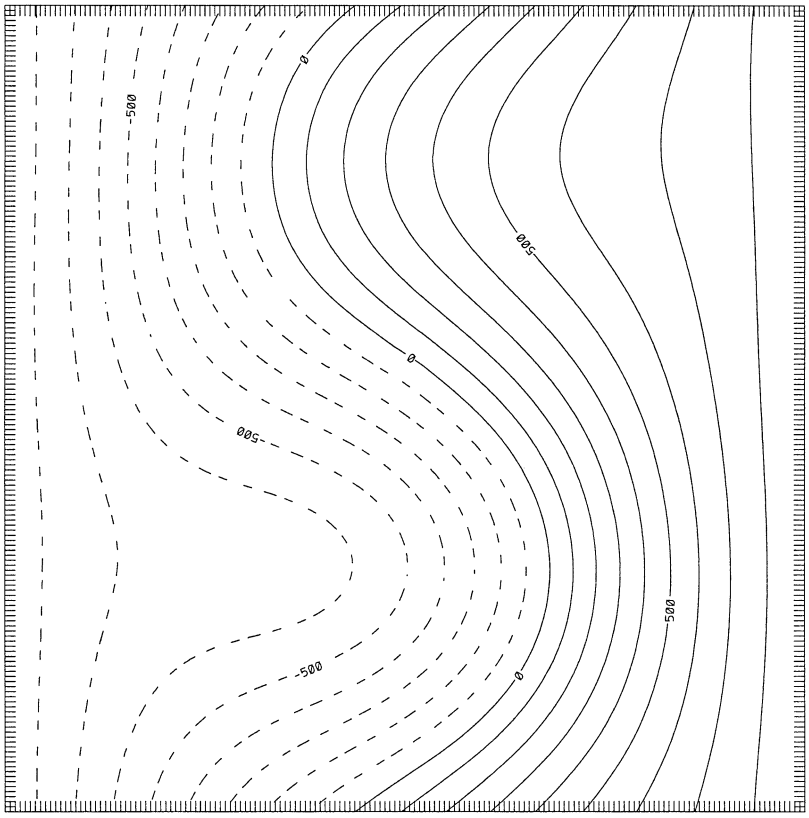

FIG. 8. The channel model pressure p at $z = 3$ km and $t = 3$ h. The length of a side of the square domain is 2000 km and the contour interval is 100 kg m^{-1} s^{-2}.

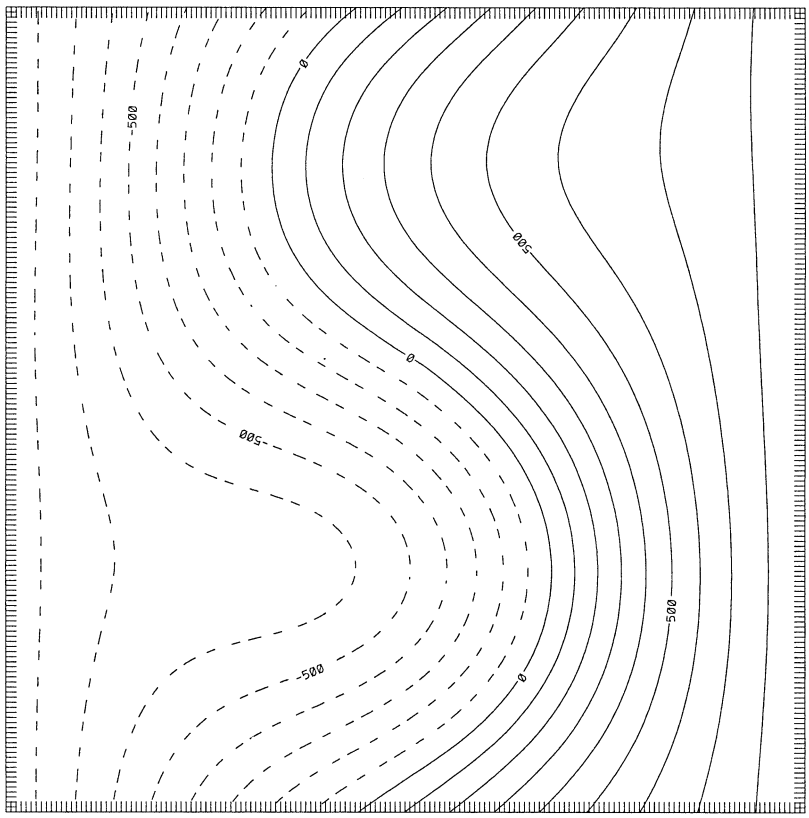

FIG. 10. The open boundary model balanced pressure p at $z = 3$ km and $t = 3$ h. The length of a side of the square domain is 2000 km and the contour interval is 100 kg m^{-1} s^{-2}.

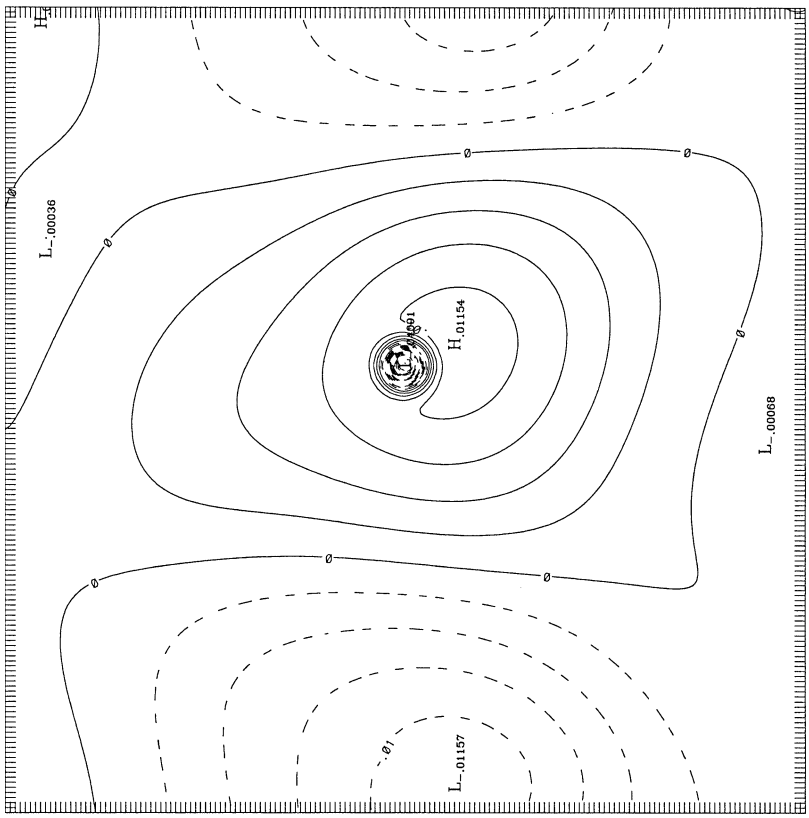

FIG. 11. The open boundary model balanced vertical velocity w at $z = 3$ km and $t = 3$ h. The length of a side of the square domain is 2000 km and the contour interval is 0.0025 m s^{-1}.

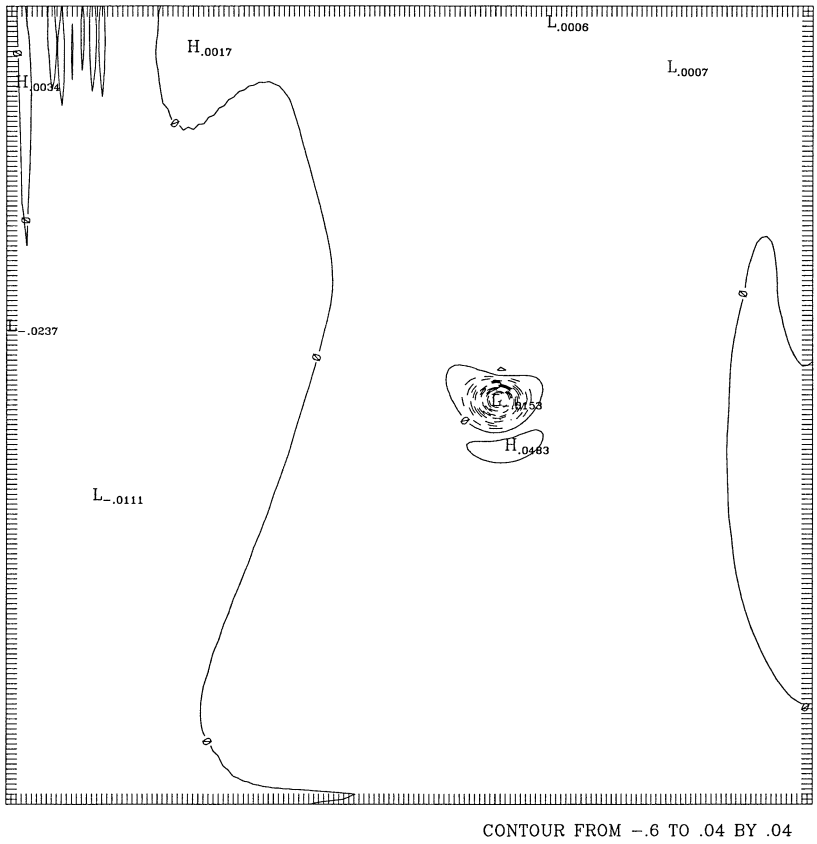

FIG. 12. The open boundary model vertical velocity w at $z = 3$ km and $t = 6$ h. The length of a side of the square domain is 2000 km and the contour interval is 0.04 m s^{-1}.

shown in Figs. 2 and 3. The two-dimensional elliptic equations for u, v, and p were solved using the routine HWSCRT from FISHPACK (Swarztrauber et al. 1975) and the three-dimensional elliptic equation for w was solved using MUDPACK (Adams 1989).

The mesoscale heating (as defined in Browning and Kreiss 1997) is

$$H = -0.50e^{-(x-u_0t-0.5X)^2/r_e^2}e^{-(y-0.5Y)^2/r_e^2} \times \sin(2\pi z/z_T)e^{-(t-6\times3600)^2/(2\times3600)^2}, \quad (6.2)$$

where $u_0 = 10$ m s^{-1} and $r_e = 50$ km. The mesoscale heating is a Gaussian bell in space (with an e-folding parameter r_e) times a full sine wave in z times a Gaussian bell in time (with an e-folding parameter of 2 h). It initially is centered at the middle of the domain and translates in the x direction in time with a speed u_0. Figures 4–6 show the fields ζ, p, and w at $z = 3$ km and $t = 6$ h obtained from the channel model version of the well-posed multiscale model. The impact of the mesoscale heating is clearly evident in these figures.

All variables from the channel model were saved on disk at 3 h. Figures 7–9 show the channel model fields ζ, p, and w at $z = 3$ km at $t = 3$ h. In addition, all variables at the lateral boundaries $x = 0$ and $x = X$ for 3 h $\leq t \leq$ 6 h were saved on disk. (Actually only the inflow variables need be saved on the lateral boundaries. But in practice, the number of inflow variables at a given lateral boundary point can change in time so that it is easier to save all variables at the lateral boundaries and then form the appropriate inflow variables at a given lateral boundary point at a given point in time.) When the variables from the channel model at $t = 3$ h were used as initial data for the open boundary model using the accurate and stable numerical approximations discussed in the appendix, the channel solution was reproduced extremely accurately just as in the shallow water case (Browning and Kreiss 1982). The channel model vorticity at $t = 3$ h was used as input to the limited-area version of the BDT initialization package applied over the same domain and with the same mesh used for the channel model (for easier comparison of fields). Figures 10–11 show the limited-area balanced fields p and w at $z = 3$ km and $t = 3$ h obtained by solving the BDT elliptic constraints (4.4b) and (4.8) with the appropriate open boundary conditions taken from section 5. Note the similarity between the limited-area balanced fields in the latter figures and the corresponding channel model fields at $t = 3$ h in Figs. 8–9. The well-posed limited-area version of the multiscale model was started from the limited-area balanced data.

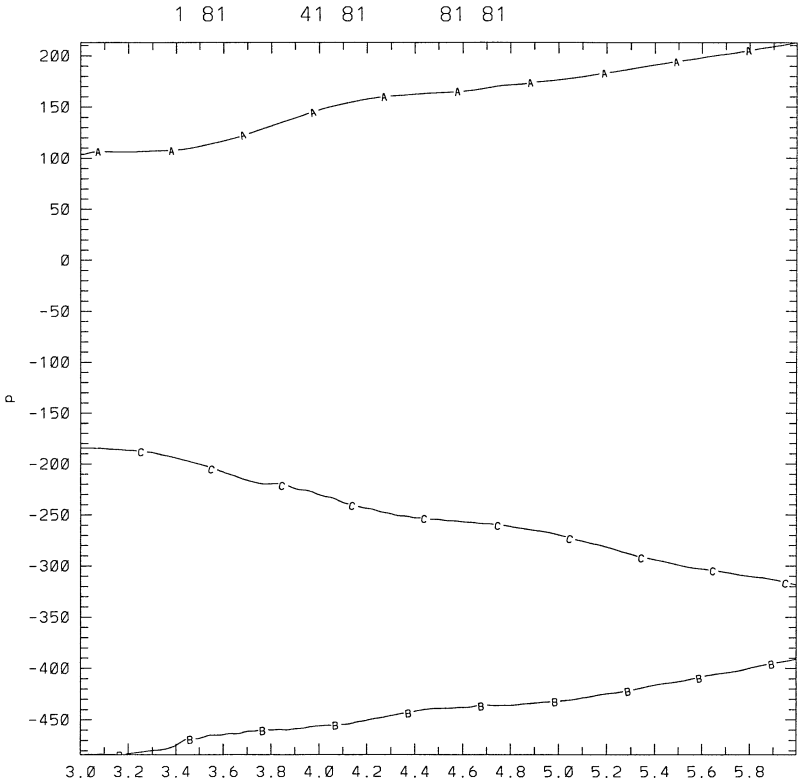

FIG. 13. The open boundary model pressure p as a function of time at the three grid points A = (0, 80, 3), B = (40, 80, 3), and C = (80, 80, 3). The abscissa is time (hours) and the ordinate is pressure (kg m^{-1} s^{-2}).

Figure 12 shows the multiscale limited-area model field w at $z = 3$ km and $t = 6$ h and this result should be compared with the corresponding channel model field in Fig. 6. Define the relative l_2 error in the field q by

$$E(q) = \|q_c - q_l)\|/\|q_c\|,$$

where the subscript c denotes a channel model field, the subscript l denotes a limited-area model field, and the norm is the standard l_2 norm. Then at $t = 6$ h, $E(p) = 0.01$ and $E(w) = 0.10$. Thus the contour plot of the limited-area model pressure at $t = 6$ h is indistinguishable from the channel model pressure at $t = 6$ h shown in Fig. 5. The larger error in w is reasonable given the skewing in the system (Browning and Kreiss 1990) and the difference between the balanced initial fields p and w computed from the limited-area version of the BDT initialization package at $t = 3$ h and the corresponding channel model fields at that time [also see discussion pertaining to this issue in Browning et al. (1997)]. Figure 13 shows the time variation of the pressure at the three grid points A = (0, 80, 3), B = (40, 80, 3), and C = (80, 80, 3). This plot shows that the initialization procedure for the open boundary model is working very well.

The same series of tests was run at the equator with similar results. At the equator $f = \beta y$ so the ellipticity of the operator in the equation (4.8) for w breaks down. However, near the equator (4.8) still provides the correct balance between w and H. At the equator the change of variables $w = H + w'$ was made in (4.8) and the value of f near the equator set to a small value so that the elliptic solver would not stop due to the ellipticity problem. Although convergence was not achieved, the value of w' was small and the result of reconstructing w resulted in an accurate approximation of the balanced value. Because the change of variable can be used anywhere on the globe, the initialization procedure is globally applicable.

It should be noted that the same resolution was used in both models for clarity of presentation. In practice, a limited-area model uses a smaller grid spacing than its global counterpart in order to resolve the small-scale features that cannot be resolved by the global model. In previous applications of the Bounded Derivative Theory and in the above set of experiments, the continuum elliptic initialization constraints were solved by the most efficient numerical methods available and the resulting data produced a slowly evolving solution in a model using an unrelated numerical approximation of the evolution equations. Thus if one uses a numerical method that is sufficient to accurately approximate the continuum equations of motion for the scales in the domain of interest, a difference in resolution between the models is not a problem.

7. Conclusions

The applicability of bounded derivative initialization to the case when heating terms with different space and timescales are present in an arbitrary domain on the globe has been demonstrated. There are many advantages of this approach. The requisite boundary conditions for the elliptic constraints that must be satisfied by a slowly evolving solution arise naturally from the well-posed boundary conditions for the three-dimensional hyperbolic system. This compatibility between the boundary conditions ensures that the solution of the hyperbolic system will evolve on the slow timescale (Browning and Kreiss 1982). Also Kreiss (1979) has shown that any scheme that leads to a slowly evolving solution will satisfy the same constraints as the scheme obtained from the bounding of an appropriate number of time derivatives. In particular, this means that any initialization scheme will have to satisfy the elliptic constraints derived in section 4. The most efficient way to solve the constraints is to use fast elliptic solvers, for example, fast Fourier transforms and/or multigrid iterative methods. Any other method, for example, digital filtering (Lynch 1985), will be much less efficient in solving these constraints. And once the initial vorticity and a heating parameterization are provided, all other variables are determined by the initialization constraints. Any inconsistencies in these remaining variables can be immediately tracked back to inaccuracies in the initial vorticity data and/or the physical parameterizations, that is, there are no complicated intervening processes to confuse the source of the problem. This already has proven invaluable in tracking down conceptual errors in various physical parameterizations.

Acknowledgments. The work of G.L.B. was supported by the Air Force Office of Scientific Research Grant F49620-98-1-0191. The authors wish to express their appreciation to Nita Fullerton for her technical editing, Paul Schultz for his internal review, Geoff Vallis for his assistance with the review process, and Bennert Machenhauer for his helpful comments on the original version.

APPENDIX

Numerical Model Details

To describe the numerical approximation of the dimensional version of the multiscale system for the open boundary case, consider the finite-difference grid $G = \{i\Delta x, j\Delta y, k\Delta z, n\Delta t : 0 \le i \le I, 0 \le j \le J, 0 \le k \le K, n \ge -1\}$, where I, J, and K are the number of grid intervals in the x, y, and z directions, Δx, Δy, and Δz are the corresponding grid increments, and Δt is the time step. The standard notation $u^n_{i,j,k}$ is used to denote the value of a grid function at the point (x_i, y_j, z_k, t_n) and missing subscripts or superscripts imply the nominal value of the missing variable. Define the finite-difference operators

$$D_t \equiv (T_{+t} - T_{-t})/(2\Delta t), \tag{A.1a}$$

$$D_x \equiv \begin{cases} [-T^2_{+x} + 4T_{+x} - 1.5(T_{+t} + T_{-t})]/(2\Delta x), \\ \qquad\qquad i = 0, \\ (T_{+x} + T_{-x})/(2\Delta x), \quad 1 \le i \le I - 1, \\ -[-T^2_{-x} + 4T_{-x} - 1.5(T_{+t} + T_{-t})]/(2\Delta x), \\ \qquad\qquad i = I, \end{cases} \tag{A.1b}$$

$$D_y \equiv \begin{cases} [-T^2_{+y} + 4T_{+y} - 1.5(T_{+t} + T_{-t})]/(2\Delta y), \\ \qquad\qquad j = 0, \\ (T_{+y} + T_{-y})/(2\Delta y), \quad 1 \le j \le J - 1, \\ -[-T^2_{-y} + 4T_{-y} - 1.5(T_{+t} + T_{-t})]/(2\Delta y), \\ \qquad\qquad j = J, \end{cases} \tag{A.1c}$$

$$D_z \equiv \begin{cases} [-T^2_{+z} + 4T_{+z} - 1.5(T_{+t} + T_{-t})]/(2\Delta z), \\ \qquad\qquad k = 0, \\ (T_{+z} + T_{-z})/(2\Delta z), \quad 1 \le k \le K - 1, \\ -[-T^2_{-z} + 4T_{-z} - 1.5(T_{+t} + T_{-t})]/(2\Delta z), \\ \qquad\qquad k = K, \end{cases} \tag{A.1d}$$

where T_{+d} and T_{-d} are the standard forward and backward translation operators along the d axis. Note the change in the definition of a finite-difference approximation of a spatial derivative at a boundary to ensure stability for the initial-boundary value problem (Gustafsson et al. 1972). The second-order finite-difference approximation of the multiscale system is given by

$$D_t s + uD_x s + vD_y s + wD_z s - \tilde{s}(w - H) = 0, \tag{A.2a}$$

$$D_t u + uD_x u + vD_y u + wD_z u + \rho_0^{-1} D_x p - fv = 0, \tag{A.2b}$$

$$D_t v + uD_x v + vD_y v + wD_z v + \rho_0^{-1} D_y p + fu = 0, \tag{A.2c}$$

$$D_t w + uD_x w + vD_y w + wD_z w + \alpha(\rho_0^{-1} D_z p_z + \tilde{p}p + gs) = 0, \tag{A.2d}$$

$$D_t p + uD_x p + vD_y p + wD_z p + wp_{0z} + \gamma p_0 (D_x u + D_y v + D_z w) = 0, \tag{A.2e}$$

where $f = f_0 + \beta y$ and $\alpha = (\Delta z/\Delta x)^2$. If the values of the grid functions at $n = -1$ and $n = 0$ are known, then (A.2) can be used to consecutively determine the values of the grid functions at $n > 0$. Note that at the boundaries the inflow variables are assumed given and the values of the outflow variables are determined from the appropriate combinations of values from (A.2). Then the values of the original variables can be determined from the inflow and outflow variables (Browning and

Kreiss 1982). The numerical approximations were computed with $I = J = 160$, $K = 12$, and $\Delta t = 10$ s.

REFERENCES

Adams, J., 1989: MUDPACK: Multigrid Fortran software for the efficient solution of linear elliptic partial differential equations. *Appl. Math. Comput.,* **34,** 113–146.

Baer, F., 1977: Adjustment of initial conditions required to suppress gravity oscillations in nonlinear flows. *Beitr. Phys. Atmos.,* **50,** 350–366.

——, and J. Tribbia, 1977: On complete filtering of gravity modes through non-linear initialization. *Mon. Wea. Rev.,* **105,** 1536–1539.

Browning, G., and H.-O. Kreiss, 1982: Initialization of the shallow water equations with open boundaries by the bounded derivative method. *Tellus,* **34,** 334–351.

——, and ——, 1986: Scaling and computation of smooth atmospheric motions. *Tellus,* **38A,** 295–313.

——, and ——, 1987: Reduced systems for the shallow water equations. *J. Atmos. Sci.,* **44,** 2813–2822.

——, and ——, 1990: An accurate hyperbolic system for approximately hydrostatic and incompressible oceanographic flows. *Dyn. Atmos. Oceans,* **14,** 303–332.

——, and ——, 1997: The role of gravity waves in slowly varying in time mesoscale motions. *J. Atmos. Sci.,* **54,** 1166–1184.

——, ——, and J. Oliger, 1973: Mesh refinement. *Math. Comput.,* **27,** 29–39.

——, A. Kasahara, and H.-O. Kreiss, 1980: Initialization of the primitive equations by the bounded derivative method. *J. Atmos. Sci.,* **37,** 1424–1436.

——, ——, and W. H. Schubert, 2000: The role of gravity waves in slowly varying in time tropospheric motions near the equator. *J. Atmos. Sci.,* **57,** 4008–4019.

Charney, J. G., 1948: On the scale of atmospheric motions. *Geofys. Publ.,* **17,** 1–17.

——, 1955: The use of the primitive equations of motion in numerical prediction. *Tellus,* **7,** 22–26.

Gustafsson, B., H.-O. Kreiss, and A. Sundström, 1972: Stability theory of difference approximations for mixed initial boundary value problems. II. *Math. Comput.,* **26,** 649–686.

Hinkelmann, K., 1951: Der mechanismus des meteorologischen Lärmes. *Tellus,* **3,** 285–296.

——, 1959: Ein numerisches experiment mit den primitiven Gleichungen. *The Atmosphere and Sea in Motion. Rossby Memorial Volume,* Rockefeller Institute Press, 509 pp.

Kreiss, H.-O., 1979: Problems with different time scales for ordinary differential equations. *SIAM J. Num. Anal.,* **16,** 980–998.

——, 1980: Problems with different time scales for partial differential equations. *Commun. Pure Appl. Math,* **33,** 399–440.

Lynch, P., 1985: Initialization of a barotropic limited-area model using the Laplace transform technique. *Mon. Wea, Rev.,* **113,** 1338–1344.

Machenhauer, B., 1977: On the dynamics of gravity oscillations in a shallow water model, with applications to normal mode initialization. *Beitr. Phys. Atmos.,* **50,** 253–271.

Phillips, N. A., 1956: The general circulation of the atmosphere: A numerical experiment. *Quart. J. Roy. Meteor. Soc.,* **82,** 123–164.

Smagorinsky, J., 1963: General circulation experiments with the primitive equations. Part I: The basic experiment. *Mon. Wea. Rev.,* **91,** 99–164.

Swarztrauber, P., and R. Sweet, 1975: Efficient FORTRAN subprograms for the solution of elliptic partial differential equations. NCAR Tech. Note TN/IA-109, 139 pp.